

EARTH
RESOURCES
LABORATORY

42 Carleton Street • Cambridge, MA 02142 • (617) 253-8027 • FAX (617) 253-6385

November 13, 1997

(OSP 65065)

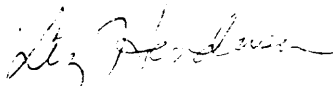
Dr. Mark A. Gilbertson, EM-52
U.S. Department of Energy
Director, Office of Science and Risk Policy
Room 5A-031
1000 Independence Avenue, SW
Washington, DC 20585-0002

Ref: DE-FG07-96ER 14705

Dear Dr. Gilbertson:

Enclosed is a copy of the Annual Progress Report and a copy of DOE Form 1332.15 for the above referenced grant.

Sincerely,



Liz Henderson for
M. Nafi Toksöz, P.I.

Encl:

cc: R. Hirsch, Office of Biological and Environmental Research/DOE (1)
N. Woodward, Office of Basic Energy Sciences/DOE (1)
R. Van De Pitte, OSP/MIT (L)
J. O'Brien, Energy Lab/MIT (L)

**IMAGING AND CHARACTERIZING THE WASTE
MATERIALS INSIDE AN UNDERGROUND STORAGE TANK
USING SEISMIC NORMAL MODES**

ANNUAL PROGRESS REPORT

for Period September 15, 1996-September 14, 1997

Xiaojun Huang, Roger Turpening, and Zhenya Zhu

**Earth Resources Laboratory
Department of Earth, Atmospheric, and Planetary Sciences
Massachusetts Institute of Technology
Cambridge, Massachusetts 02139**

November 1997

Prepared for

**THE U.S. DEPARTMENT OF ENERGY
AGREEMENT NO. DE-FG07-96ER14705**

NOTICE: This report was prepared as an account of work sponsored by the United States Government. Neither the United States nor the Department of Energy, nor any of their employees, nor any of their contractors, subcontractors, or their employees, makes any warranty, express or implied, or assumes any legal liability or responsibility for the accuracy, completeness, or usefulness of any information, apparatus, product or process disclosed or represents that its use would not infringe privately-owned rights.

ABSTRACT

This report covers the initial year of investigation of the normal modes of oscillation of underground storage tanks. This work is directed toward finding a way to estimate the properties of the waste in tanks on the Hanford Reservation with the minimal use of instrumentation in a tank.

Theoretical work, as well as laboratory-sized physical modeling was undertaken this first year and the satisfying corroboration between the two methods has given us confidence to go forward. The physical model results presented here are for a tank containing a single layer of liquid wastes, while the theoretical formulation is valid for both the single-layer and multi-layer cases. Given this solid foundation we proceed to tanks containing multiple layers of solids.

TABLE OF CONTENTS

ABSTRACT	ii
INTRODUCTION	1
OVERVIEW OF METHODS	1
USING NORMAL MODES OF VIBRATION	3
NORMAL MODES OF A BURIED TANK	4
Numerical Modeling	4
Theory	4
PHYSICAL MODELS	17
DISCUSSION	20
WORK SCHEDULED FOR YEAR TWO	21
SUMMARY	22
REFERENCES	22

INTRODUCTION

The storage of hazardous wastes in underground tanks (USTs) is a common practice. An extreme example can be found at the Hanford Facility in Washington state, where 177 large tanks (Figure 1) have been storing hazardous radioactive and toxic wastes for a long time. 149 tanks are single-shell tanks and 28 are double-shell. 67 of the single-shell tanks are “assumed leakers” and for this reason the liquid contents of those tanks has been pumped into double-walled tanks. In addition, this pumping operation has been extended to the remaining single-shell tanks with the result that the single-shell tanks primarily contain moist solid waste, while the double-shell tanks contain primarily liquids with a salt cake crust.

It is important to know the structure of the wastes to avoid surprises during the sampling operations, and to properly prepare for the eventual transfer of the waste materials. It is equally important that any survey of the contents of the tanks be done in a cost-effective and timely manner. This research effort is directed towards that end.

OVERVIEW OF METHODS

The Hanford tanks have several risers that penetrate the roof of the tank and provide access to the interior. In every tank one of those risers contains a liquid observation well (LOW), while the remaining risers only provide access to the surface of the wastes.

The methods for direct sampling of the wastes are well developed at Hanford. There are “push” devices and coring tools for retrieving samples in the solid wastes and additional tools for obtaining samples of sludge. However, they suffer from the problem common to all coring/sampling methods, namely that they are point measurements. While they give a great deal of information about a single point in the waste mass, they yield nothing about the overall characterization of the wastes. Furthermore, the current sampling methods can only operate directly beneath a riser, therefore no information of any type exists in “off-riser” locations.

All of the geophysical methods applied to the earth (seismic, radar, electromagnetic techniques, etc.) have at some time been proposed for use inside the single-shell Hanford tanks. This train of thought is appropriate since the materials in the single-shell tanks are earth-like in consistency, whereas the double-shell tanks contain primarily liquids. However, the only known use of a geophysical technique in a Hanford tank was done by Turpening *et al.* (1995) who used the crosswell seismic method between two LOWs in tank

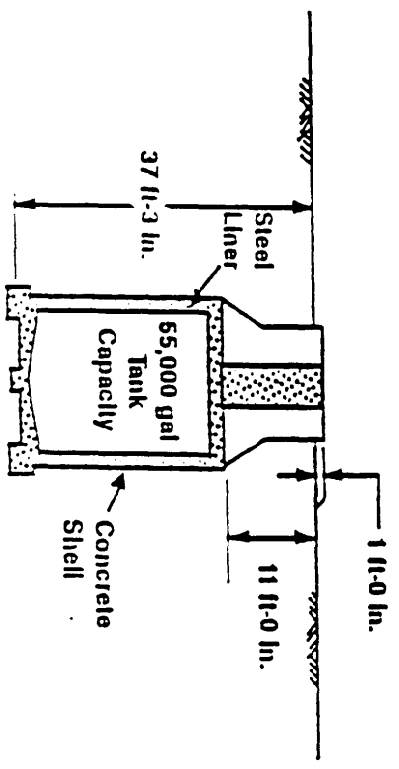
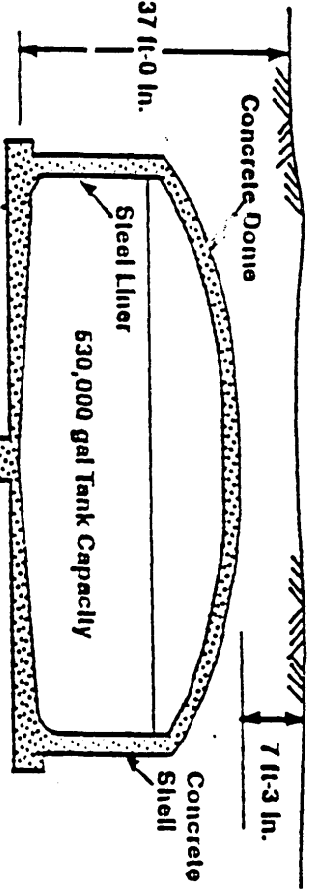
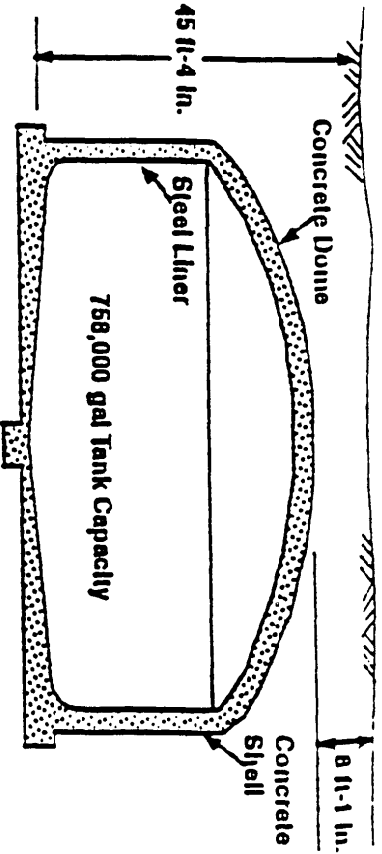
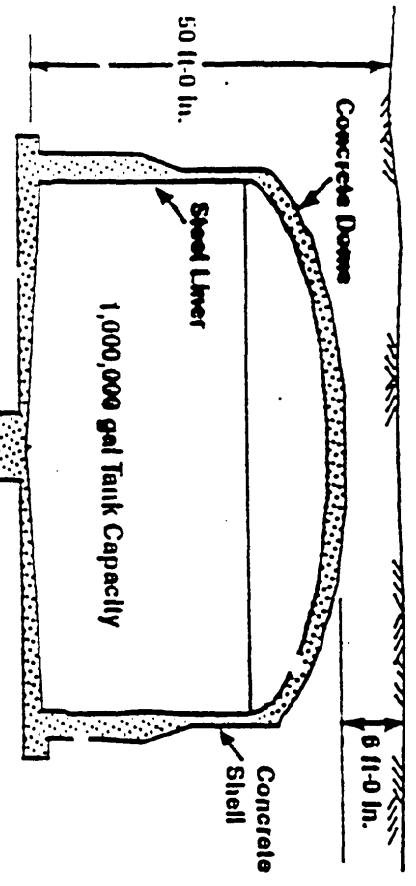
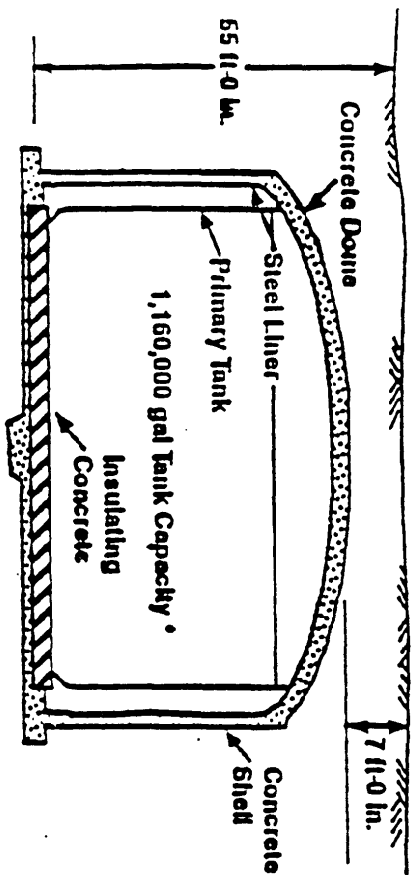


Figure 1: Cross-section sketches of the various styles of underground tanks on the Hanford Reservation.

114TX. The value of this method is limited, however, because very few tanks at the Hanford Facility have two LOWs.

Although there is only one LOW in each tank, there are several risers that allow access to the wastes. Therefore, two separate strings of instrumentation could be used in a tank if a stand-alone method of deployment could be found for, say, the seismic source. A cone penetrometer would be one such method of deploying a source into a tank even if that tank contained solid waste materials. Currently, there is no seismic source that has been designed for a CPT string, nor is there a CPT string designed to accept a seismic source.

The reverse is common but undesirable in this case. There are CPT strings that do contain a seismic receiver, but this requires that the source be placed in the LOW. When the source is activated it creates strong tube waves which complicate the already difficult problem of imaging the contents of a tank.

USING NORMAL MODES OF VIBRATION

Free oscillations (normal modes) of the whole earth were first predicted by Lamb in 1879 and Love in 1911, but it was not until 1952 that any were observed. At that time, investigators (e.g. Backus and Gilbert, 196 1; Gilbert and Dziewonski, 1975; Tanimoto **and** Bolt, 1983) began to predict the nature of higher modes of oscillation, however the early computers limited them to analytical solutions. This in turn limited them to the spherically-symmetrical properties of the earth.

As computers became more powerful it became possible to numerically model some of the higher-mode free oscillations that are sensitive to an aspherical earth, anisotropy in the inner core (e.g., Woodhouse and Wong, 1986), and anisotropy in the upper mantle (Mochizuki, 1986; Park, 1993).

Observations have also improved such that now 1500 of the roughly 2000 modes with periods greater than 80 seconds have been identified in seismic data.

Because the M.I.T. Earth Resources Laboratory (ERL) possesses a massively parallel computer (nCUBE with 512 nodes and 100 gigabytes of disc space), we are transferring this academic interest in free oscillations to practical use at the Hanford Facility.

NORMAL MODES OF A BURIED TANK

Given the constraint of a single LOW in each tank, it is appropriate to turn to the use of the normal modes of tank vibration as a way to estimate the nature of the wastes contained in a tank. This is because the normal modes can be generated by a source on the surface outside the tank and observed by sensors (e.g., hydrophones) in the one LOW. Furthermore, since the source is on the surface, we can use it to generate normal modes in several tanks simultaneously thereby speeding up the survey process manifold. Obviously, one must have a string of receivers in each of the tanks when the source is activated.

To speed up our investigation of normal modes, we are undertaking both a theoretical effort and a solid-scale modeling effort during this first year.

Numerical Modeling

In our first year we have looked at those cases where analytical solutions are possible. Although this means that the source is assumed to be inside a tank with the receivers, the insight gained is valuable.

A tank is assumed to contain a liquid, although it can be a multi-layered liquid. Therefore the acoustic wave equation is the one that must be solved. We recognize that the single-shell tanks contain solids and we will move forward to solid waste and the elastic wave equation after our understanding of normal modes of a tank are established.

The parameters used in our numerical and physical modeling closely approximate the dimensions of a single-shell tank at the Hanford Site (Figure 1).

Theory

The Acoustics of Fluid in a Cylindrical Tank

The wave equation in the fluid in terms of displacement potential is

$$\nabla_f^2 \nabla^2 \Phi - \ddot{\Phi} = 0.$$

The general solution to the wave equation in cylindrical coordinate is in the form as below,

$$\Phi = \sum_n J_n(k_n r) e^{in\theta} (A_n \cos k_z z + B_n \sin k_z z).$$

Accordingly, the radial and axial partial displacement U_r and U_z , and the pressure distribution of the wave field will be,

$$\begin{aligned}
U_r &= \frac{\partial \Phi}{\partial r} \quad , \\
U_z &= \frac{\partial \Phi}{\partial z} \quad , \\
P &= \rho_f \omega^2 \Phi \quad .
\end{aligned}$$

We assume that the shell of the tank may be considered as rigid boundary, while the fluid surface can be taken as free surface. Therefore, at the boundaries, we have

$$\begin{aligned}
U_r|_{r=R} &= 0 \quad , \\
U_z|_{z=0} &= 0 \quad , \\
P|_{z=h} &= 0 \quad .
\end{aligned}$$

If we design the experiment in such a way that only axially symmetric motion can be excited. the wave field described by displacement potential will be,

$$\Phi = \sum_{\mathbf{l}} \sum_{\mathbf{n}} A_{\mathbf{l},\mathbf{n}} J_0(k_{r,\mathbf{l}} r) \cos(k_{z,\mathbf{n}} z) \quad .$$

Due to boundary condition restrictions, only the characteristic standing waves can exist. The characteristic wavenumber of the standing waves are,

$$\begin{aligned}
k_{z,\mathbf{n}} &= \frac{\pi}{h} (n + \frac{1}{2}) \quad , n = 0, 1, 2, \dots \\
k_{r,\mathbf{l}} &= \frac{\text{root}_l[J_1(x)]}{R} \quad , l = 0, 1, 2, \dots
\end{aligned}$$

Correspondingly, the characteristic frequencies of these modes are,

$$\omega_{\mathbf{l},\mathbf{n}} = V_f \sqrt{k_{z,\mathbf{n}}^2 + k_{r,\mathbf{l}}^2}$$

There is a low cutoff frequency of the standing wave field, from which the height of the fluid inside the tank can be obtained.

$$\begin{aligned}
f_c &= \frac{\omega_c}{2\pi} = \frac{V_f}{4h} \quad , \\
h &= \frac{V_f}{4f_c} \quad .
\end{aligned}$$

Figures 2 and 3 display purely vertical motion. these were computed in the high frequency band shown because we will compare these with small physical models later in the report.

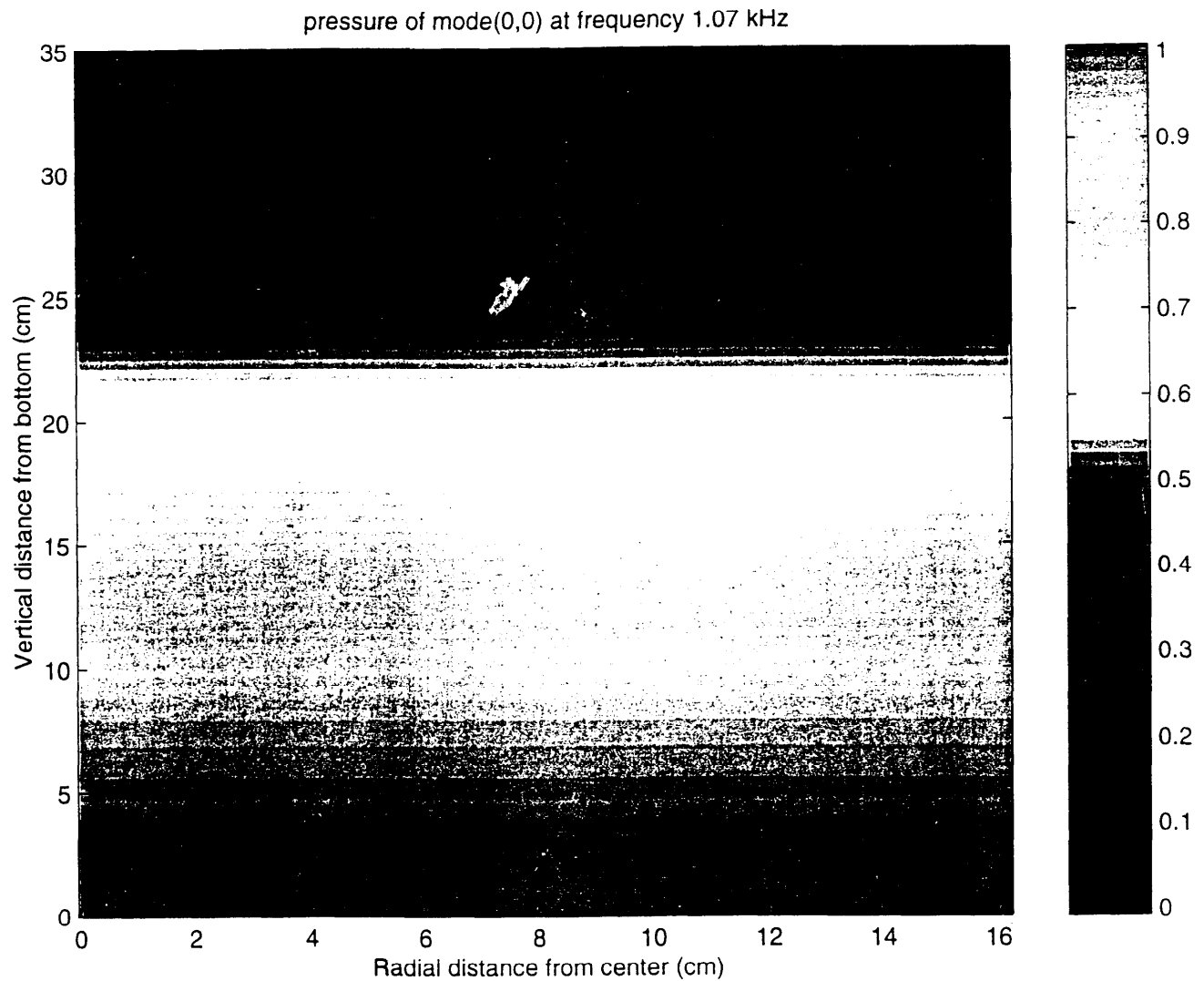


Figure 2: Numerically-modeled pressure field in one-half of a small model tank at a frequency of 1.07 kHz. The dimensions of the tank were taken to approximate the size of the small lab-sized model used in the physical modeling experiment. This mode represents purely vertical wave propagation in the tank. In a full-size Hanford tank, this mode would exist at approximately 14 Hz. This mode was not seen in the model experiments because the instrumentation used there had low sensitivity at this frequency.

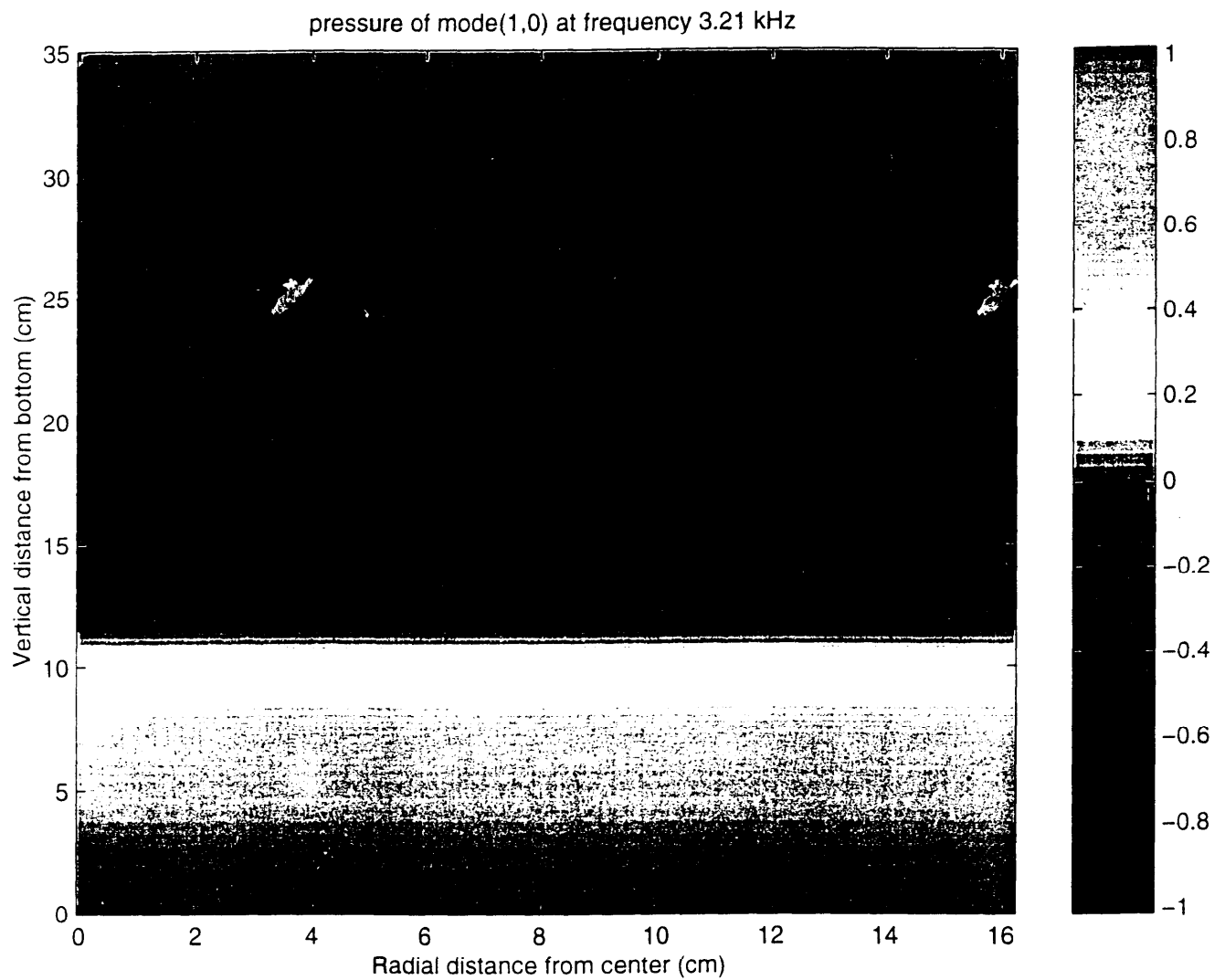


Figure 3: Numerically-modeled pressure field in one-half of a small model tank at a frequency of 3.21 kHz. This mode is also purely vertical and would scale to approximately 43 Hz in a Hanford tank. Note that it is assumed here that the liquid completely fills the tank, which does not occur in the Hanford tanks.

The Acoustics of Multi-Layered Fluids in a Cylindrical Tank

When the fluid inside the tank is multi-layered, without the source term, the wave equation for each of the individual layers is,

$$\nabla_i^2 \nabla^2 \Phi_i - \ddot{\Phi}_i = 0, \quad i=1, 2, 3, \dots, n.$$

Similar to the single layered fluid case, the wave field in each layer can be represented as,

$$\Phi_i = J_0(k_r r) [A_i \cos(k_i z) + B_i \sin(k_i z)],$$

where,

$$\overline{\nabla_i^2} = k_r^2 + k_i^2.$$

In axial direction, the actual wave field will be the one that couples the individual layers together by matching the axial boundary conditions as follows,

$$U_{z_i} \Big|_{z_i=0} = 0 \quad (\text{rigid bottom})$$

$$P \Big|_{z=h} = 0 \quad (\text{free surface})$$

$$\left. \begin{aligned} P_j \Big|_{z=h_j} &= P_{j+1} \Big|_{z=h_j} \\ U_{z_j} \Big|_{z=h_j} &= U_{z_{j+1}} \Big|_{z=h_j} \end{aligned} \right\} \quad (\text{at interface } j)$$

By matching the boundary condition in axial direction, a characteristic equation can be obtained, which is shown below,

$$|c| = 0,$$

where c is a $2n$ by $2n$ matrix, and its elements are listed in the appendix. It is a function of k_1, k_2, \dots, k_n . For convenience, we rewrite the above equation as,

$$f(k_1, k_2, k_3, \dots, k_n) = 0$$

In each of the layers,

$$\frac{\omega^2}{\nabla_i^2} = k_i^2 + k_{r,i}^2,$$

therefore, k_2, k_3, \dots, k_n can be expressed as a function of k_1 ,

$$\left\{ \begin{array}{l} k_2 = \sqrt{\frac{V_1^2}{V_2^2}(k_1^2 + k_{r,1}^2) - k_{r,1}^2} \\ k_3 = \sqrt{\frac{V_1^2}{V_3^2}(k_1^2 + k_{r,1}^2) - k_{r,1}^2} \\ \dots\dots\dots \\ k_n = \sqrt{\frac{V_1^2}{V_n^2}(k_1^2 + k_{r,1}^2) - k_{r,1}^2} \end{array} \right.$$

If we substitute the above expressions back to the characteristic equation, the characteristic equation becomes only a function of k_1 . A set of solutions can be obtained through numerical computation. The characteristic frequencies of the standing wave field can be denoted as,

$$\omega_{1,m} = V_1 \sqrt{k_{1,m}^2 + k_{r,1}^2} \quad 1, m = 1, 2, 3, \dots$$

The total wave field is the linear combination of all the modes, which is,

$$\Phi_i = \sum_1 \sum_m J_0(k_{r,1}r) [A_{1,m} \cos(k_{1,m}z) + B_{1,m} \sin(k_{1,m}z)].$$

When a point source is present in the tank at the position of $(r_0, 0, z_0)$ via one of the risers at the roof of the tank, which is off-axis, the wave equation at the source layer will be,

$$V_f^2 \nabla^2 \Phi - \ddot{\Phi} = -\frac{q(t)}{\rho_f} \delta(r - r_0) \delta(z - z_0)$$

where $q(t)$ is the source pressure output. We denote the Fourier transformation of the right-hand side of the above equation as $f_0(\omega, r, z)$, which represents the source excitation. Since the standing wave modes constitute an orthogonal as well as complete basis, we may project the source excitation term onto the basis, and the coefficient $B_{1,n}$ at each base component reflects the fraction of energy that the source contributes to that certain mode.

$$f_0(\omega, r, z) = \sum_I \sum_n B_{1,n} J_0(k_{r,1}r) \cos(k_{z,n}z),$$

$$B_{1,n} = -\frac{2\pi r_0 Q(\omega) J_0(k_{r,1}r_0) \cos(k_{z,n}z_0)}{\rho_f \frac{R^2}{z'} J_0^2(k_{r,1}R) \frac{h}{2}}$$

Assuming the source is in the p -th layer, by substituting the source term and the wave field expression back to the wave equation at the p -th layer. the wave field distribution at the source layer can then be solved.

$$\Phi_p = \sum_I \sum_m -\frac{8\pi r_0}{\rho_p R^2 (h_p - h_{p-1})} \frac{J_0(k_{r,1}r_0) J_0(k_{r,1}r)}{J_0^2(k_{r,1}R)} \frac{Q(\omega)}{\omega^2 - \omega_{1,m}^2} \cos(k_{p,m}(z - z_0)).$$

Therefore, the pressure distribution should be,

$$P_p = \omega^2 \rho_p \Phi_p = -\frac{8\pi r_0}{R^2(h_p - h_{p-1})} \frac{J_0(k_{r,l}r_0)J_0(k_{r,l}r)}{J_0^2(k_{r,l}R)} \frac{Q(\omega)}{1 - (\frac{\omega_{l,m}}{\omega})^2} \cos(k_p(z_m - z)).$$

Using the relations built by boundary matching in axial direction, the wave fields in other layers can be easily obtained.

Figures 4-9 are examples of computations using this multi-layer algorithm. here, both radial and axial motion are seen. Again, the high frequency band was chosen to facilitate comparison with small physical models later in the report.

Detection of Velocity Structure in a Tank

Based on the above derivation. we propose a measurement which can detect the velocity structure of the tank fluid. The source and receiver are to be in the same layer. Choosing the neighboring axial modes (which have zero radial components) in the spectrum of the received signal, the axial wavenumber can be simplified as

$$k_p = \frac{\omega}{V_p}.$$

If we denote the two neighboring characteristic frequencies as ω_1 and ω_2 , and the corresponding measured acoustic pressures as P_{p_1} and P_{p_2} , a link between the two measurement properties can be built by the above theory.

$$P_{p_1} \propto Q(\omega_1) \cos(k_{p_1}(z - z_0))$$

$$P_{p_2} \propto Q(\omega_2) \cos(k_{p_2}(z - z_0))$$

where $Q(\omega)$ is the source spectrum. and $z - z_0$ is the known source-receiver vertical separation. The above relations can be rewritten in terms of velocity and divide one by another,

$$\frac{P_{p_1}}{P_{p_2}} = \frac{\cos[\frac{\omega_1(z - z_0)}{V_p}] Q(\omega_1)}{\cos[\frac{\omega_2(z - z_0)}{V_p}] Q(\omega_2)}$$

where only V_p is unknown. At the region of $[0, \pi]$, the above equation will have unique solution for V_p . Also the minimum pressure P_{p_0} is measured at a frequency ω_0 located in between ω_1 and ω_2 . Therefore the thickness of the layer can be obtained by the following formula.

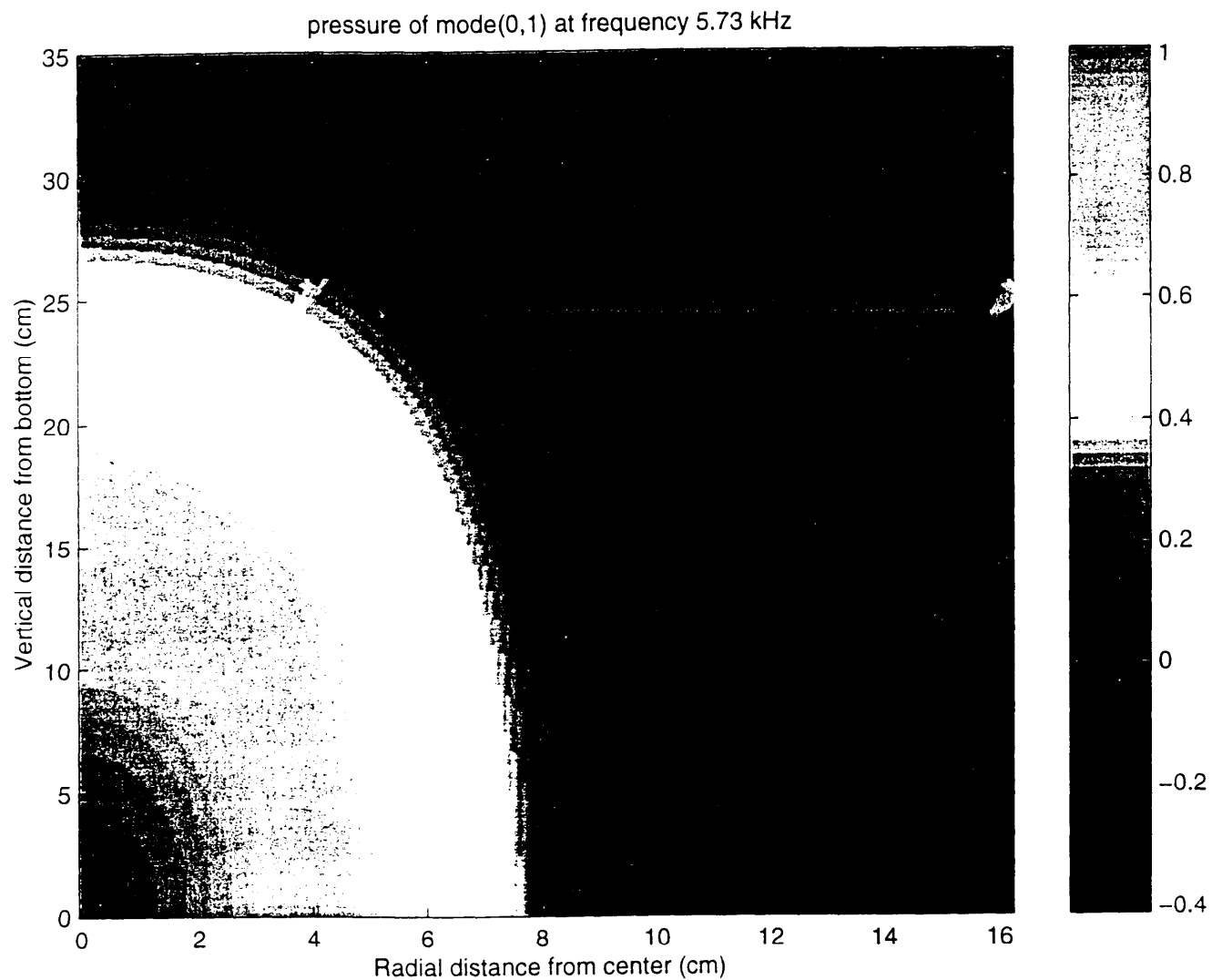


Figure 4: Numerically-modeled pressure field in one-half of a small model tank at a frequency of 5.73 kHz. This mode was observed in the model tank experiments, however the vertical variation in pressure was not observed. That occurred because here we assumed infinite rigidity of the bottom and perfectly vertical side walls; those parameters were not achieved in the physical model experiments. In a full-size Hanford tank, this mode would occur at approximately 76 Hz.

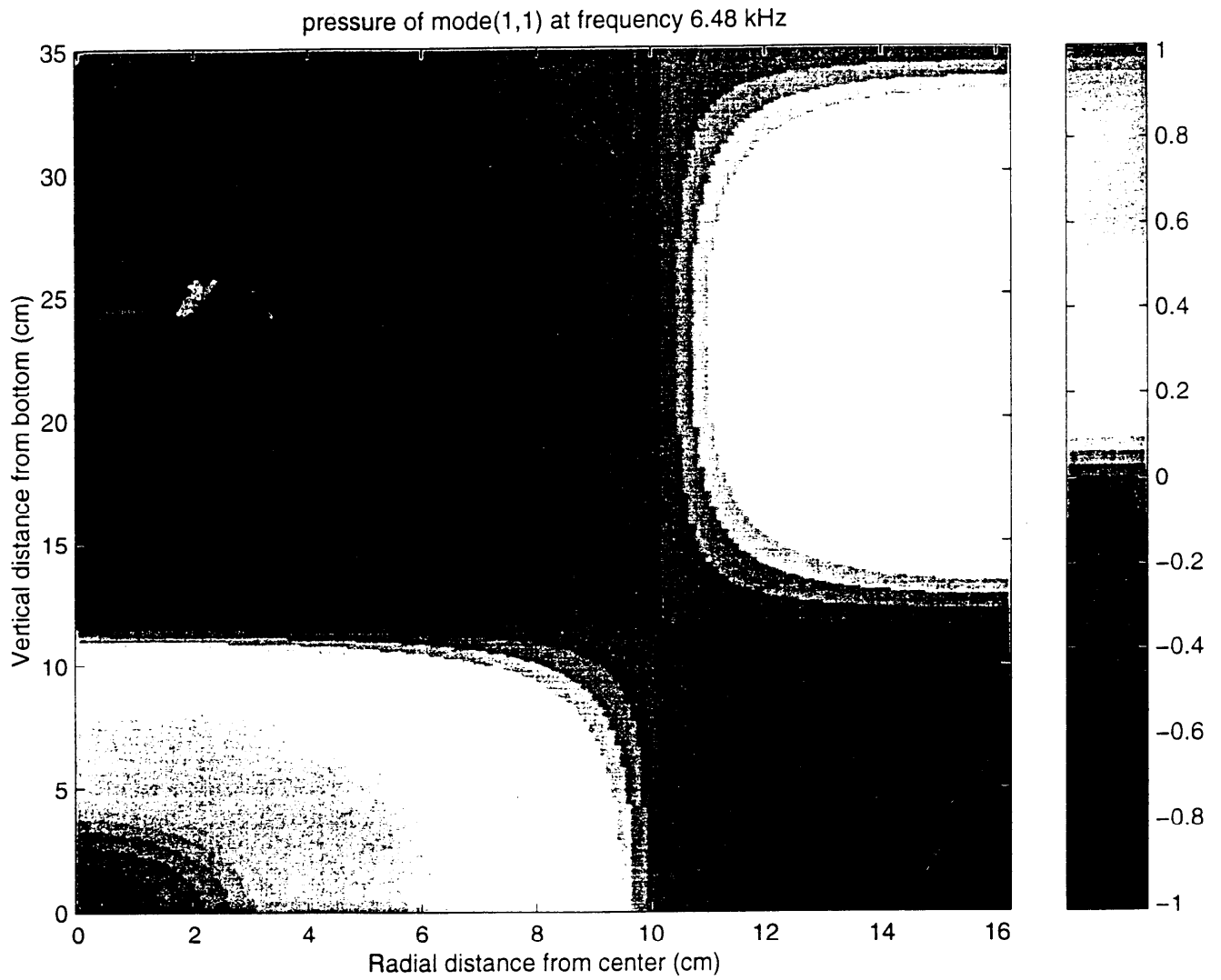


Figure 5: Numerically-modeled pressure field in one-half of a small model tank at a frequency of 6.48 kHz. This mode may have been seen in the physical model experiments but at a very low amplitude.

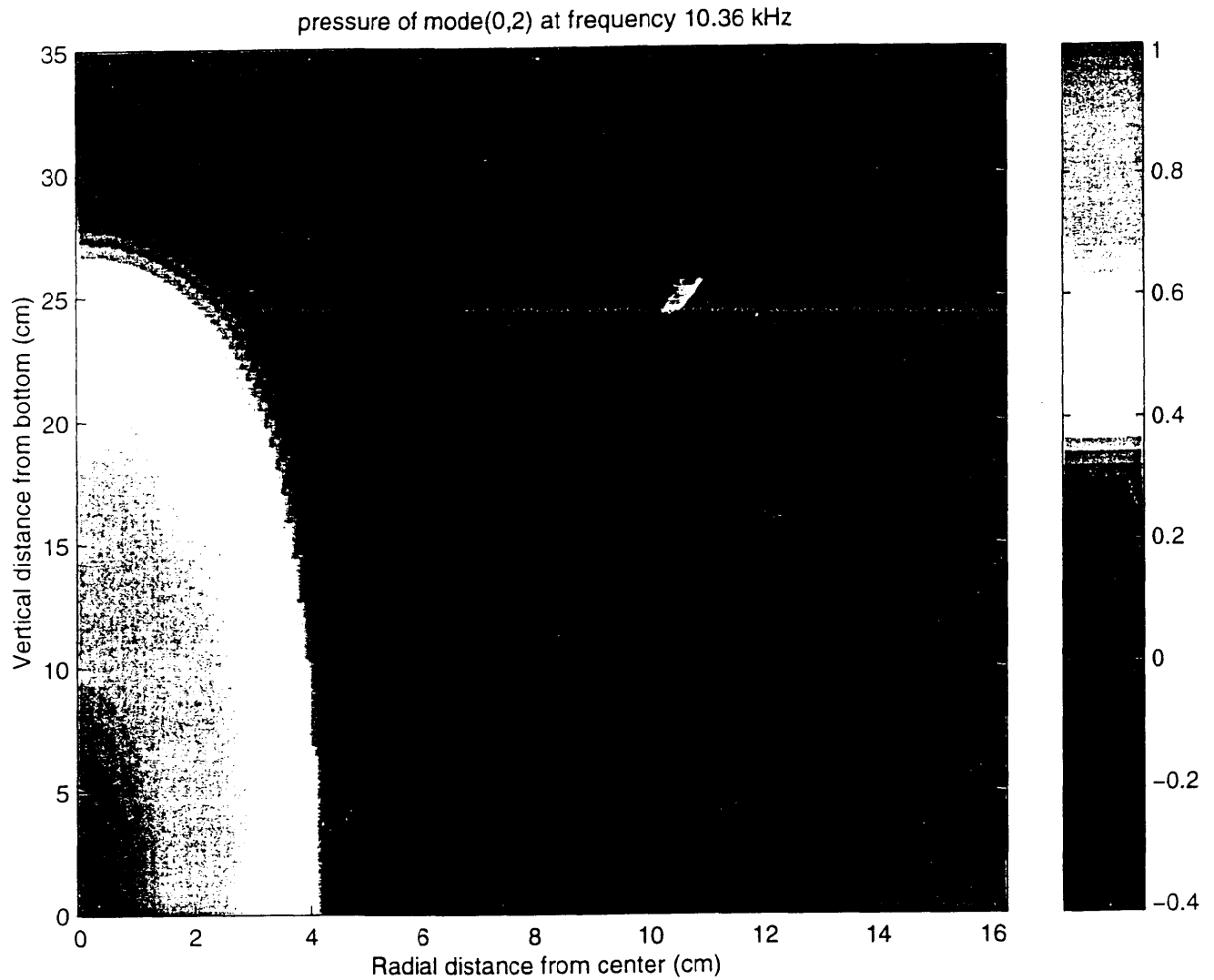


Figure 6: Numerically-modeled pressure field in one-half of a small model tank at a frequency of 10.36 kHz. This mode was seen in the physical model experiments, but again without the vertical variation in pressure. In a full-size Hanford tank, this mode would occur at 138 Hz. Remember that here it is assumed that the tank is completely full of liquid, which does not occur in the Hanford tanks.

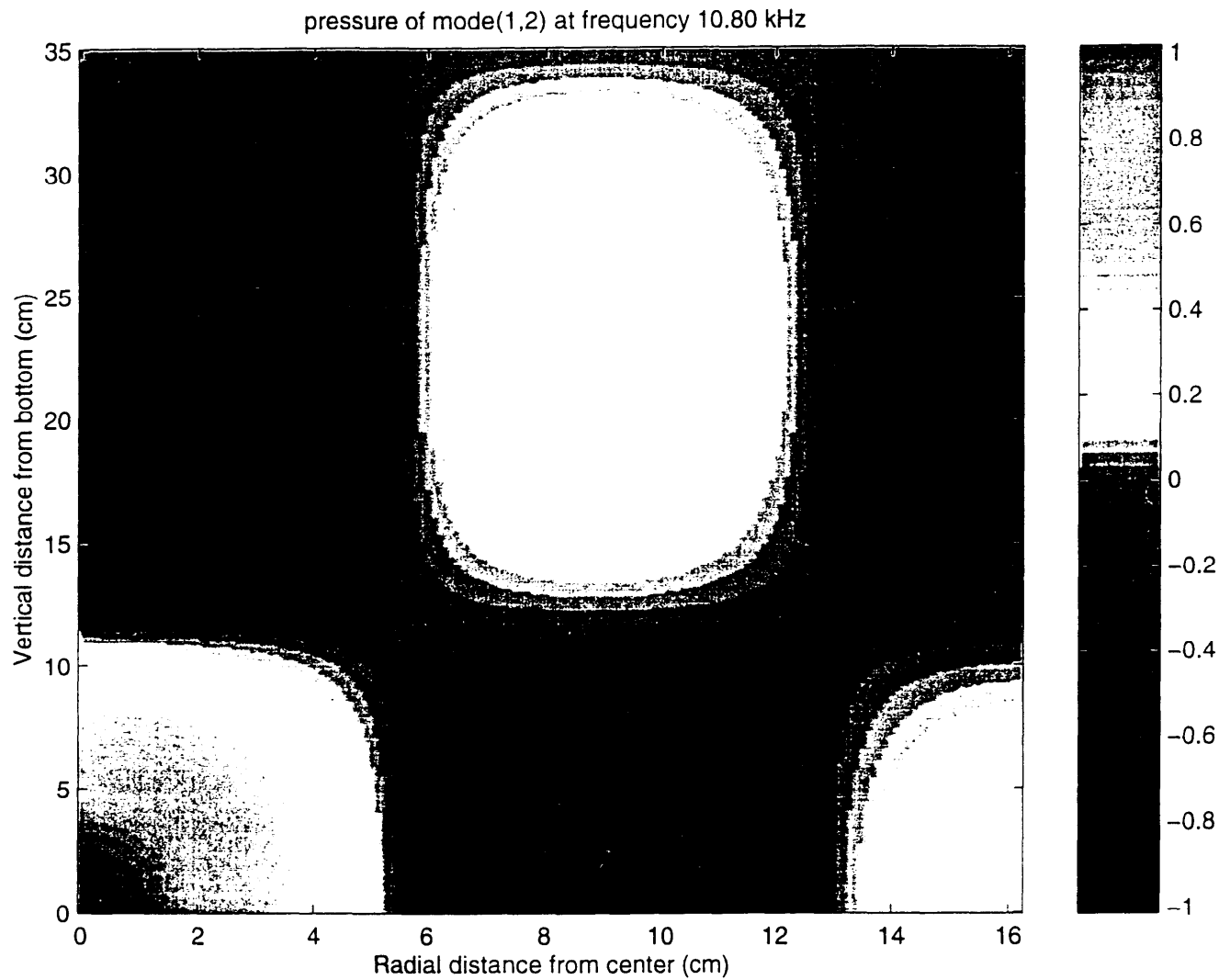


Figure 7: Numerically-modeled pressure field in one-half of a small model tank at a frequency of 10.80 kHz. This mode was also seen in the physical model experiments as a portion of the split peak in the spectra in Figure 11 at 9.64 kHz. In a full-size Hanford tank, this mode would occur at a frequency of 144 Hz.

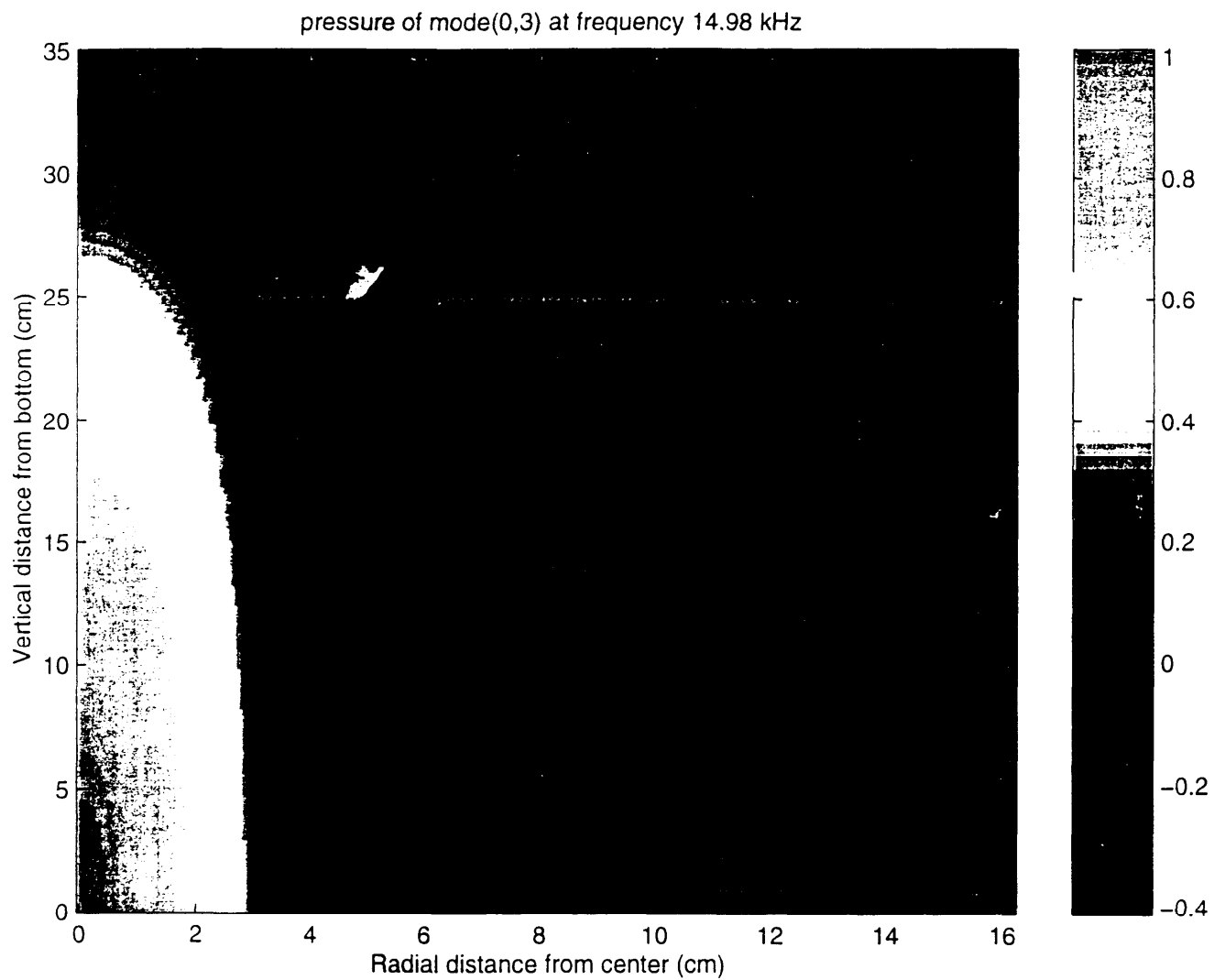


Figure 8: Numerically-modeled pressure field in one-half of a small model tank at a frequency of 14.98 kHz. This mode was not seen in the physical model experiments.

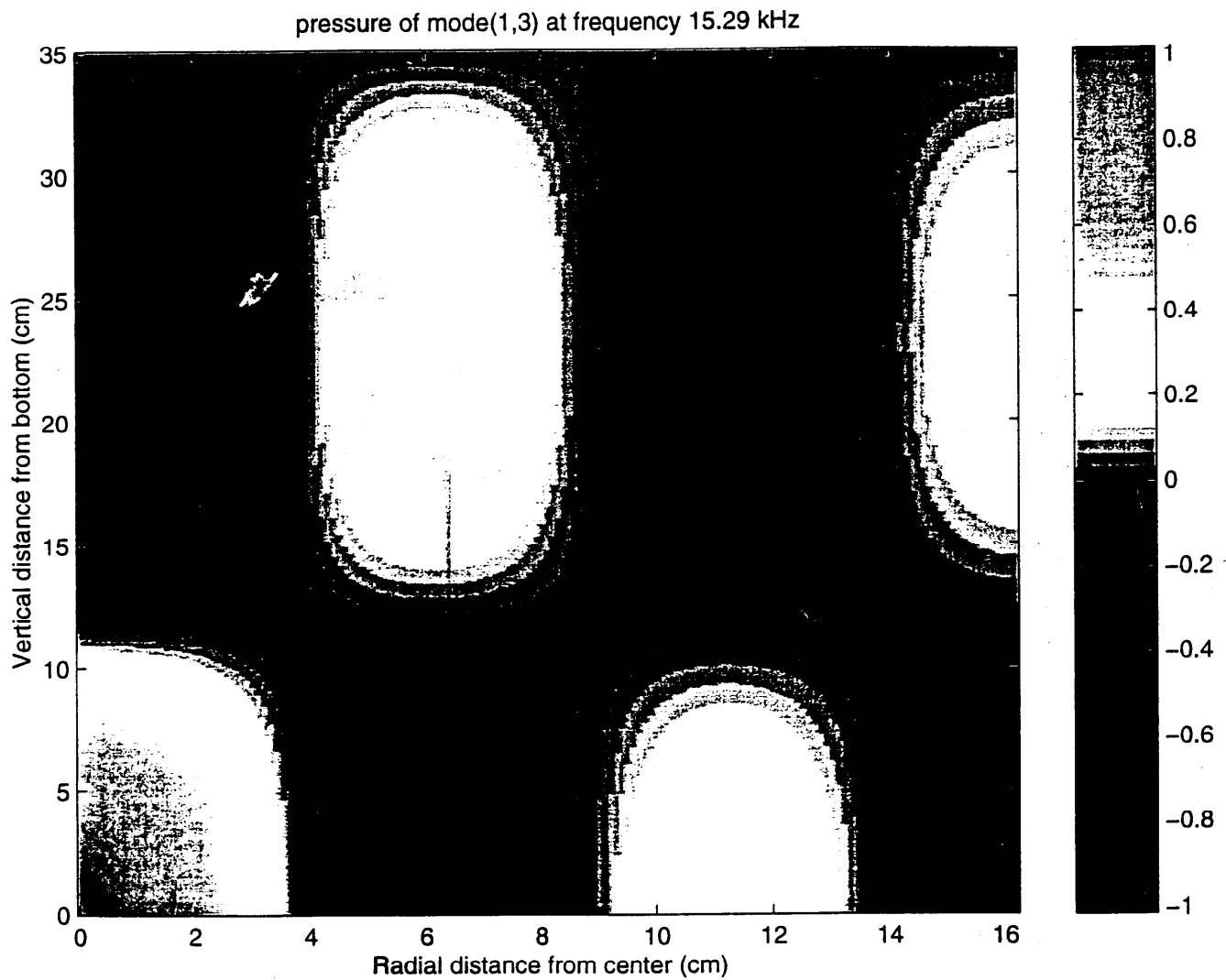


Figure 9: Numerically-modeled pressure field in one-half of a small model tank at a frequency of 15.29 kHz. This mode was seen in the physical model experiments at a frequency of 18.8 kHz. In a full-size Hanford tank, this mode would occur at approximately 250 Hz.

$$h_p - h_{p-1} = \frac{8\pi r_0}{R^2} \frac{Q(\omega_0)}{P_{p_0}} \left[\frac{\cos\left(\frac{\omega_1}{V_p}(z-z_0)\right)}{1 - \left(\frac{\omega_1}{\omega_0}\right)^2} + \frac{\cos\left(\frac{\omega_2}{V_p}(z-z_0)\right)}{1 - \left(\frac{\omega_2}{\omega_0}\right)^2} \right]$$

where R is the radius of the tank.

PHYSICAL MODELS

As a check on the numerical modeling, we built small physical models of tanks and conducted experiments in the laboratory. By scaling the frequency of the acoustic/seismic energy used in the model experiments one can maintain the same relationship between wavelength and the size of the tank as seen in the full-sized tanks. Figure 10 indicates the dimensions of the model tanks, and the location of the source and receivers (pressure) in the model tank.

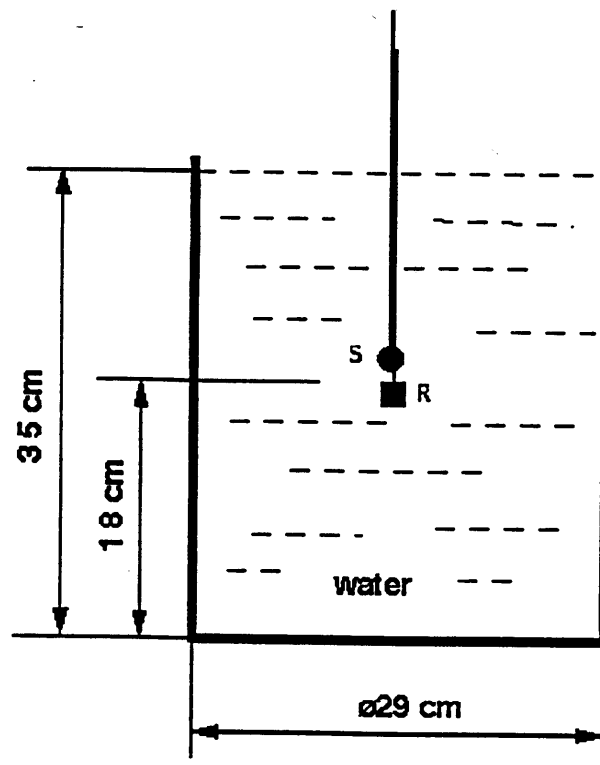


Figure 10: Diagram of the physical model arrangement simulating a Hanford tank. The pressure-sensitive receiver, R, was placed along the center line of the tank model with the source. It is displaced to the side in this diagram for clarity.

The data in 'Figure 11 was obtained by operating the source in a continuous manner at a single frequency and recording the output of the receiver. The frequency of the source is then changed by a small amount and the recording repeated. In this manner, using fine steps in frequency, the plot in Figure 11 was generated. The normal modes of vibration of the model. tank are seen as the strong responses at discrete frequencies.

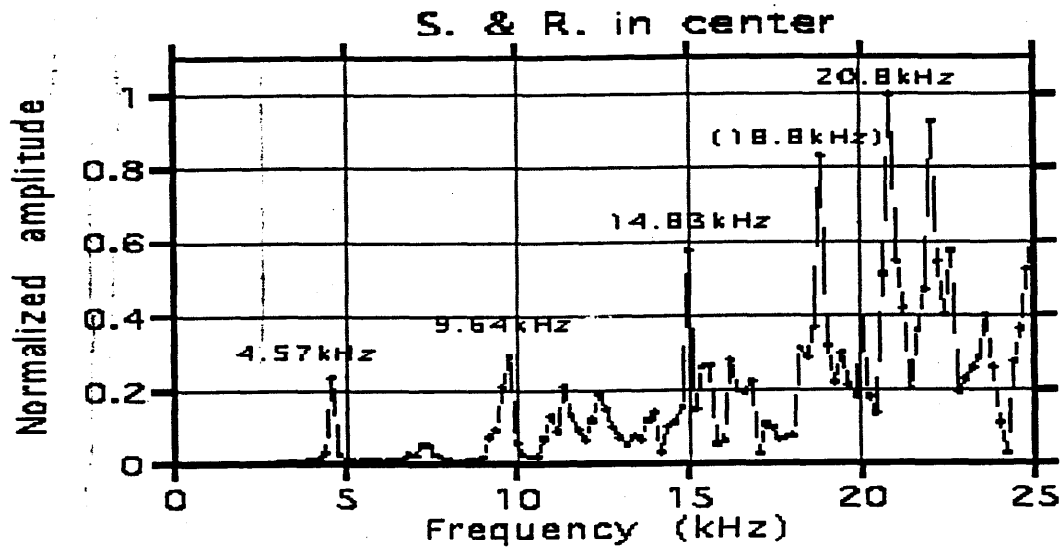


Figure 11: Plot of the response of a pressure transducer in the center of the tank model gathered while the source slowly up in frequency. The amplitude of the source output is kept constant.

Figures 12 and 13 show the response as a function of location in the tank. From these figures one can see that the two lowest frequency modes (4.57 kHz and 9.64 kHz) are essentially standing waves in the radial direction in the tank with no variation in amplitude in the vertical direction. The higher modes (14.83 kHz and 20.8 kHz) are complicated modes with both vertical and radial variations in amplitude.

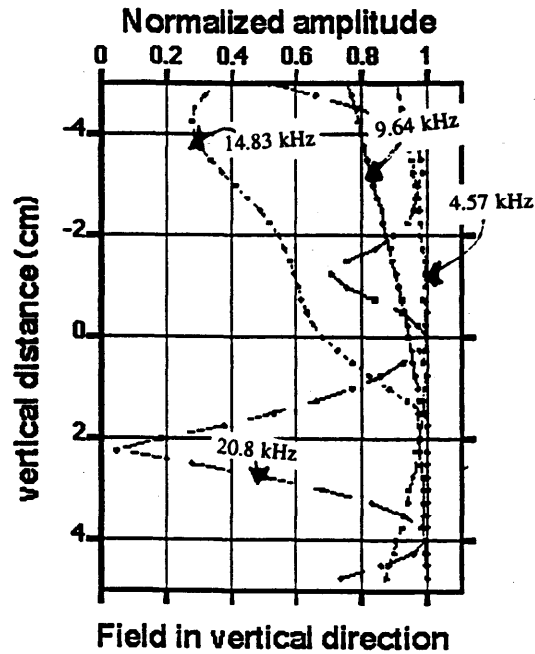


Figure 12: Amplitude of first four normal modes of oscillation as a function of position on a vertical axis through the center of the tank. Note that the first two modes (4.57 kHz and 9.64 kHz) have little or no variation along this vertical axis. Therefore these are purely radial models of vibration.

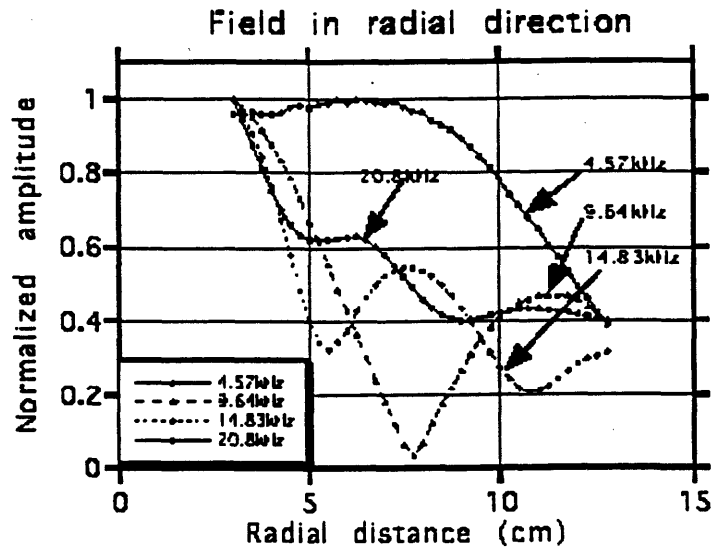


Figure 13: Radial variation in amplitude as a function of position along a radial axis at mid-depth in the tank. Note that the first model of oscillation (4.57 kHz) represents a single wavelength of acoustic energy across the tank.

Small physical models with scaled dimensions representing a Hanford tank were made to see if the theoretically predicted modes of vibration could be seen. In all cases a tank is assumed to be full of liquid waste with the properties of water and a source of acoustic energy is placed in the center of the tank.

The first measurements were taken in that configuration with a pressure transducer also in the center of the tank. The data in Figure 12 was generated while the source generated a continuous tone that was slowly moved up in frequency. A resonance response (a normal mode of vibration) of the water filled tank is clearly seen at certain discrete frequencies. The first four (4.57 kHz, 9.64 kHz, 14.83 kHz, and 20.8 kHz) normal modes have been identified on the graph.

To observe the spatial variation of pressure in a tank, a transducer is placed along the center line with the source (Figure 10) and moved from the bottom to the surface of the water. This was done while the source remained constant at one frequency selected from the modes noted in Figure 11. The pressure as function of depth is displayed in Figure 12 and one can see there that the first two modes (4.57 kHz and 9.64 kHz) display little variation as a function of depth, i.e., they appear to be purely radial modes of oscillation. The next two higher modes do exhibit variation as a function of depth.

Additional data was taken in the model tank to observe the radial variation in pressure for each of the four modes. These data are presented in Figure, 13. Here we see that all four of the modes under study do exhibit radial variation in pressure. One can visualize the lowest mode of oscillation as a single wavelength of energy across the tank. The higher modes exhibit more complex radial variation in pressure and thus the total pressure variation is not simple.

DISCUSSION

Looking at the calculated and measured normal modes together is more informative than looking at either one individually. First, we notice that the very lowest modes computed (1.07 kHz and 3.21 kHz) were not seen in the small model experiments. This is a result of the low response of the instrumentation in the model experiment in the low frequency portion of the spectrum. However, the computed modes at 5.73 kHz, 10.36 kHz, and 14.98 kHz have been identified in the physical tank model (at 4.57 kHz, 9.64 kHz, and 14.83 kHz). This is a very good fit between theory and the physical model given that the physical model does not have the strict parameters used in the theoretical formulation such as perfect rigidity of the walls and bottom.

The theoretical modes seen at 10.36 kHz and 10.80 kHz are probably those slightly lower amplitude responses seen in the physical model at approximately 11.1 kHz. Note, in fact, that in the spectra from the physical model, the peak at approximately 11.1 kHz is a split peak just as the theoretical calculations suggest (i.e., 10.36 kHz and 10.80 kHz).

The numerical modeling done in this report-used dimension parameters that approximated the size of the small physical model tank used in the laboratory. Thus the spectral peaks were seen in the kilohertz range. As observed above, we are encouraged by the comparison of the theoretically-computed modes and those that were observed in the small model of a tank.

Note that the size of the model of a tank is approximately 1/75 the size of a Hanford tank; Therefore, when the modes of oscillation are measured at Hanford we will find them in the tens to hundreds Hertz range. This bodes well for such field measurements because there are many strong vibratory seismic sources that are capable of generating long monochromatic signals.

WORK SCHEDULED FOR YEAR TWO

The excellent fit between theory and small physical model data for a singlefluid layer is encouraging and gives us confidence to move on to solid layers. In addition, we will remove the source from the tank and place it on the surface, and leave the receivers in the tank. We know that no LOW exists precisely in the center of any tank. Therefore, in all of our theoretical and physical modeling work we will move the receivers to an off-center location in a tank.

As in the case of the whole earth, the lack of symmetry in these cases forces us to use other numerical methods, namely the finite difference method, for next year's work. This in turn means that we must use our massively parallel computer.

We will extend our theoretical work to include sensitivity analyses. This will give us a feel for the sensitivity of the modal frequencies as a function of layer number and layer parameters.

SUMMARY

In this report, we have shown that the theoretical formulation for the normal modes of a liquid-filled tank are understood. We have shown that these modes display both vertical and radial variations in pressure and their complexity rises as one goes to higher and higher modes.

Laboratory-sized physical models have given us confidence that the theoretical work is correct.

REFERENCES

- Backus, G. and F. Gilbert, 1961, The rotational splitting of the oscillations of the earth, *Proceed. National Academy of Science*, **47**,3429-3439.
- Gilbert, F. and A. Dziewonski, 1975, An application of normal mode theory to the retrieval of structural parameters and source mechanisms from seismic *spectra*, *Philosophical Trans. of Roy. Soc. London*, **A287**, 187-269.
- Lamb, Sir H. L., 1879, *Hydrodynamics*, Dover Pub., 738 pp.
- Love, A.E.H., 1911, *Some Problems of Geodynamics*, Dover Pub., 180 pp.
- Mochizuki, E., 1986, The free oscillations of an anisotropic and heterogeneous earth, *Geophys. J. Roy. Astron. Soc.*, **86**, 167.
- Park, J., 1993, The sensitivity of seismic free oscillations to upper mantle anisotropy, zonal symmetry, *J. Amer. Geophys. Union*, **98**, 19,933.
- Tanimoto, T. and A. Bolt, 1983, Coupling of torsional modes in the Earth, *Geophys. J. Roy. Astron. Soc.*, **74**, 83-95.
- Turpening, R., Z. Zhu, C. Caravana, J. Matarese, and W. Turpening, 1995, Acoustic imaging of underground storage tank wastes-A feasibility study, Westinghouse Hanford Co., Richland, Washington.
- Woodhouse, J.H. and Y.K. Wong, 1986, Amplitude, phase, and path anomalies of mantle waves, *Geophys. J. Roy. Astron. Soc.*, **87**, 753.